Supplemental Information

Axo-axonic Innervation of Neocortical Pyramidal Neurons by GABAergic Chandelier Cells Requires AnkyrinG-associated L1CAM

Yilin Tai, Nicholas B. Gallo, Minghui Wang, Jia-Ray Yu, and Linda Van Aelst

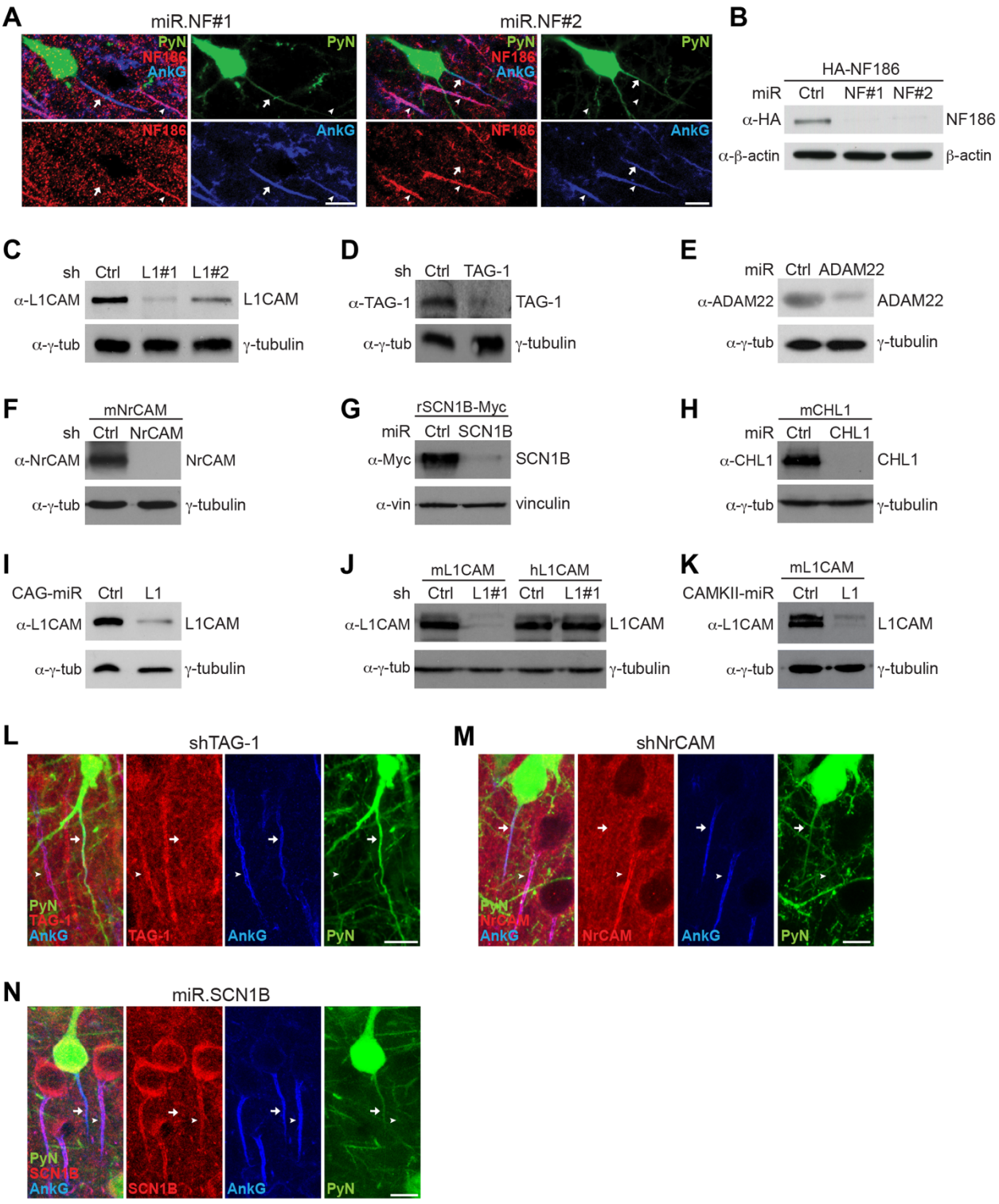

Figure S1. Validation of Constructs Used in RNAi Screening and L1CAM Knockdown and Rescue Studies. Related to Figures 1, 2, and 3.

(A, B) Validation of shRNAs against NF186. (A) Representative images of PyNs in layer II of the somatosensory cortex from CD1 mice electroporated at E15.5 with plasmids expressing EGFP and

CAG-driven miR30-based shRNAs targeting NF186 (miR.NF#1 or miR.NF#2) and sacrificed at P28. AISs and endogenous NF186 are visualized by immunostaining for AnkG (blue) and NF186 (red), respectively. GFP+ PyNs have reduced NF186 levels at their AIS (arrows) compared to neighboring GFP- PyNs (arrowheads). Scale bars, 10 μm. (B) Western blot of total lysates from HEK293T cells co-transfected with a plasmid expressing HA-tagged NF186 and one of the indicated RNAi constructs, probed with antibodies to HA and β-actin as a loading control.

(C-H) Validation of shRNAs used in RNAi screen of PyN-expressed cell surface molecules. (C) Western blot of total lysates from 10 days *in vitro* (DIV10) primary cortical neurons infected at DIV3 with lentiviruses expressing a non-targeting shRNA (shCtrl) or L1CAM-targeting shRNAs (shL1#1 or shL1#2), probed with antibodies to L1CAM and γ-tubulin as a loading control. (D) Western blot of total lysates from Neuro-2a cells transfected with a plasmid expressing shCtrl or a TAG-1-targeting shRNA (shTAG-1), probed with antibodies to TAG-1 and γ-tubulin. (E) Western blot of total lysates from DIV14 primary cortical neurons transfected via AMAXA electroporation at E15.5 (DIV0) with a plasmid expressing a CAG-driven control miR30-based shRNA (miR.Ctrl) or an ADAM22-targeting miR30-based shRNA (miR.ADAM22), probed with antibodies to ADAM22 and γ-tubulin. (F-H) Western blots of total lysates from HEK293T cells co-transfected with indicated RNAi and mouse (m) or rat (r) cDNA constructs, probed with antibodies to NrCAM (F), Myc (G), or CHL1 (H) and γ-tubulin or vinculin as a loading control.

(I) Western blot of total lysates from DIV10 primary cortical neurons infected at DIV3 with lentiviruses expressing a CAG-driven miR.Ctrl or an L1CAM-targeting miR30-based shRNA (CAG-miR.L1), probed with antibodies to L1CAM and γ-tubulin.

(J) Western blot of total lysates from HEK293T cells co-transfected with a plasmid expressing mouse L1CAM (mL1CAM) or RNAi-resistant human L1CAM (hL1CAM) and one of the indicated RNAi constructs, probed with antibodies to L1CAM and γ-tubulin.

(K) Western blot of total lysates from HEK293T cells co-transfected with a plasmid expressing mL1CAM and one of the indicated CAMKII-driven RNAi constructs, probed with antibodies to L1CAM and γ-tubulin.

(L-N) Validation of shRNAs against TAG-1, NrCAM, and SCN1B by immunofluorescence. Representative images of PyNs in layer II of the somatosensory cortex from CD1 mice electroporated at E15.5 with plasmids expressing EGFP and shRNAs targeting TAG-1 (shTAG-1) (L), NrCAM (shNrCAM) (M), or SCN1B (miR.SCN1B) (N) and sacrificed at P28. AISs and endogenous TAG-1, NrCAM, or SCN1B are visualized by immunostaining for AnkG (blue) and TAG-1, NrCAM, or SCN1B (red), respectively. GFP+ PyNs have reduced levels of the RNAi-targeted protein of interest at their AIS (arrows) compared to neighboring GFP- PyNs (arrowheads). Scale bars, 10 μm.

For all western blots, data shown are representative of three independent experiments.

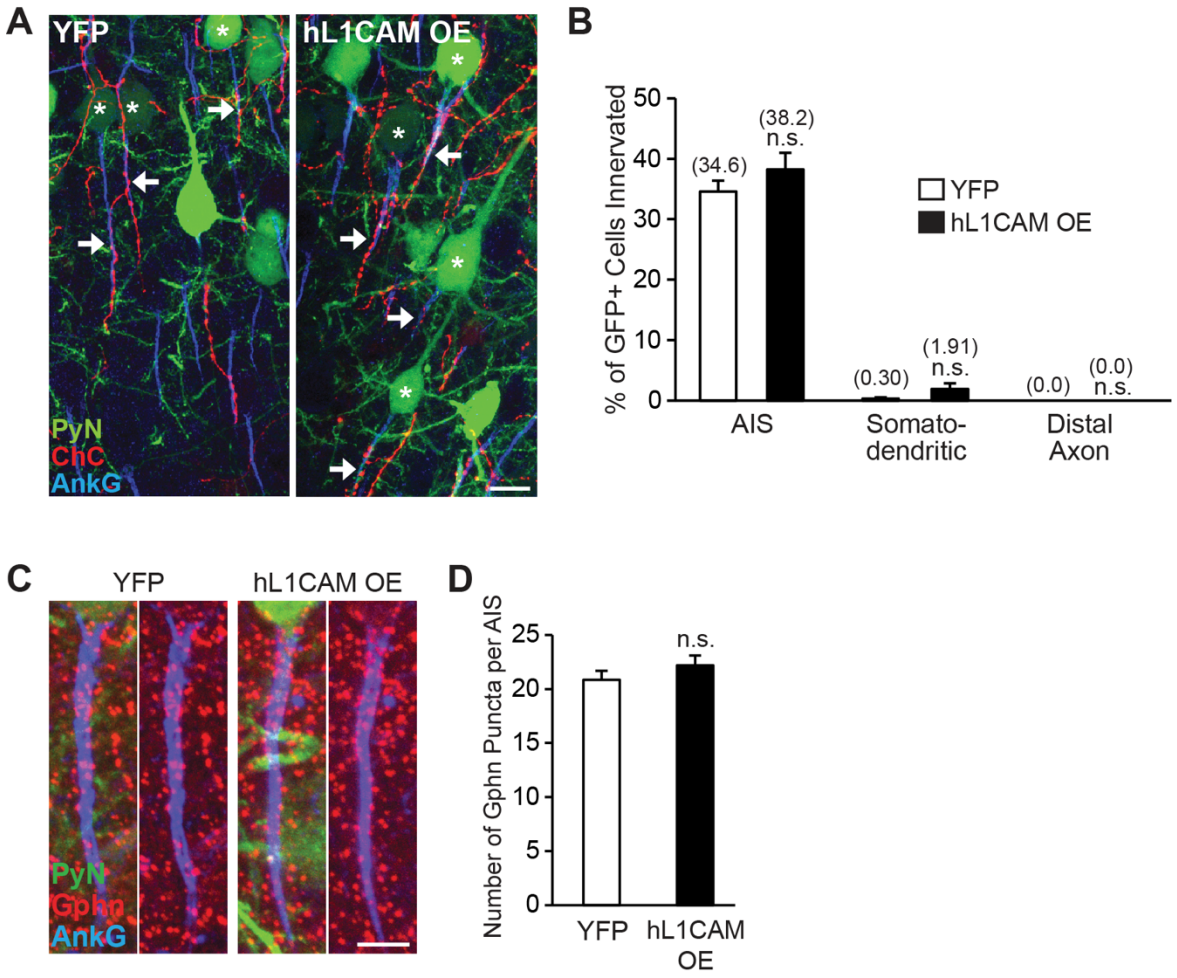

Figure S2. PyN L1CAM Overexpression Does Not Perturb ChC/PyN Synaptic Innervation or Proper Subcellular Targeting of ChC Cartridges. Related to Figure 3.

(A) Representative images of PyNs innervated by ChC cartridges in layer II of the somatosensory cortex from *Nkx2.1-CreER;Ai9* mice electroporated at E15.5 with plasmids expressing EGFP and human L1CAM (hL1CAM; overexpression (OE)) or YFP control (YFP) and sacrificed at P28. Scale bar, 10 µm.

(B) Quantification of the percentage of GFP+ PyNs innervated at their AIS, somatodendritic compartment, or distal axon (> 50 µm away from soma) by single RFP+ ChCs at P28. Innervation percentages are indicated for each condition. 10-20 ChCs and 12-111 GFP+ PyNs per ChC from 3 animals were analyzed for each condition; Student's t tests.

(C) Representative images of GFP+ PyN AISs in layer II of the somatosensory cortex from CD1 mice electroporated at E15.5 with plasmids expressing EGFP and hL1CAM (overexpression (OE)) or YFP control and sacrificed at P28. Inhibitory synapses are visualized by immunostaining for the GABAergic postsynaptic marker gephyrin (Gphn; red). Scale bar, 5 µm.

(D) Quantification of the average number of gephyrin puncta per GFP+ PyN AIS at P28. 30-33 AISs from 3 animals were analyzed for each condition; Student's t test.

For all images of ChC/PyN AIS innervation, stars and arrows indicate GFP+ PyNs innervated by RFP+ ChC cartridges and the site of GFP+ PyN AIS innervation, respectively.

n.s. (not significant) indicates $p \geq 0.05$. Data are mean ± SEM.

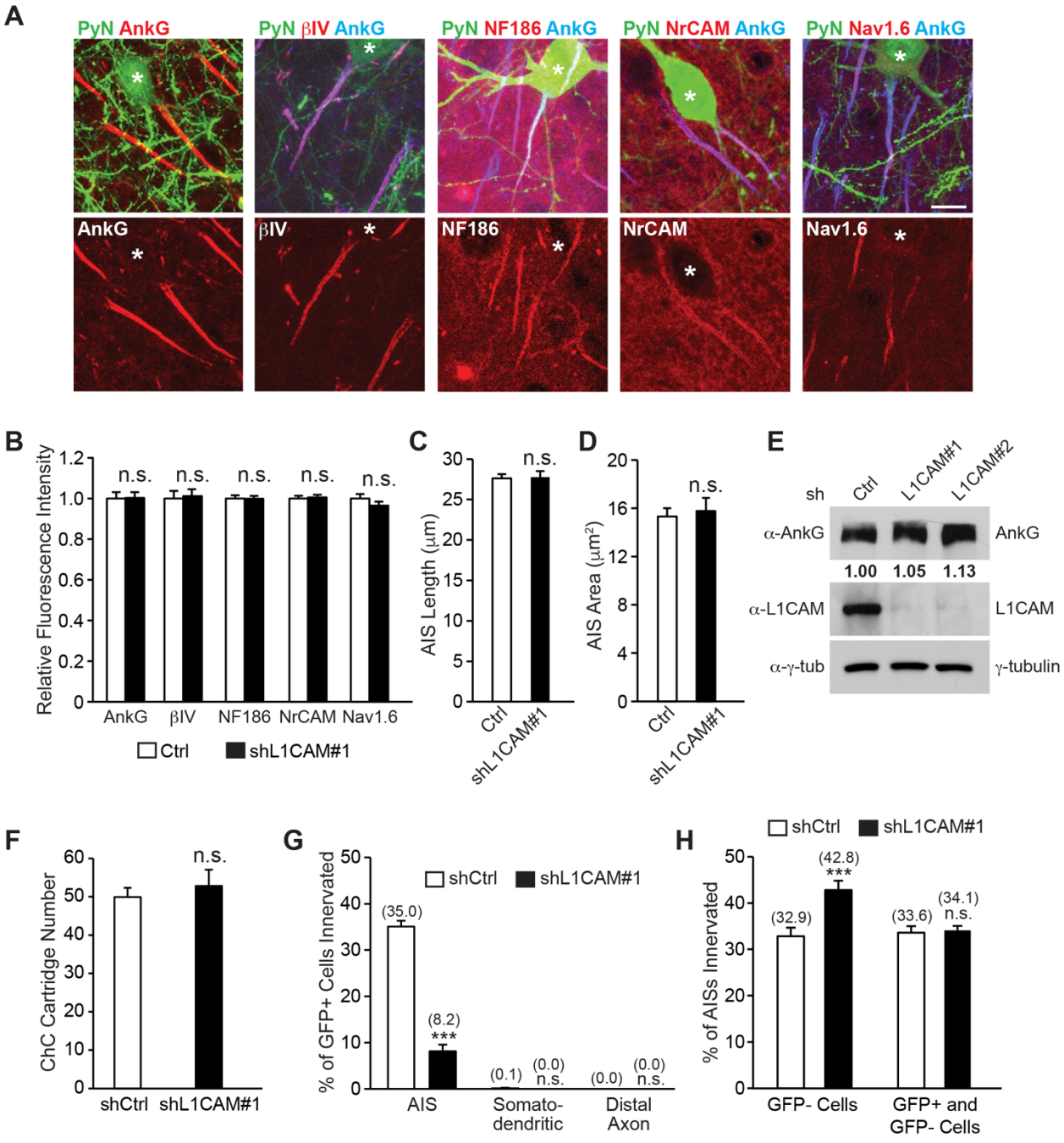

Figure S3. PyN L1CAM Knockdown Does Not Affect AIS Structure or the Expression Levels/Distribution of AIS-enriched Proteins nor the Number and Proper Subcellular Targeting of ChC Cartridges. Related to Figure 3.

(A, B) Knockdown of L1CAM in neocortical PyNs does not affect the localization or expression of AIS-enriched proteins. (A) Representative images of GFP+ PyNs (stars) and neighboring GFP- PyNs in layer II of the somatosensory cortex from CD1 mice electroporated at E15.5 with plasmids expressing EGFP and shL1CAM#1 and sacrificed at P28. Endogenous levels of proteins of interest are visualized by immunostaining for AnkG, βIV-spectrin (βIV), NF186, NrCAM, or Nav1.6.

Scale bar, 10 μm. (B) Quantification of the relative fluorescence intensity of AnkG, βIV-spectrin, NF186, NrCAM, and Nav1.6 immunostaining at the AIS of neocortical PyNs under the indicated conditions. 14-15 AISs from 3 animals were analyzed for each condition; Student's t tests.
(C, D) Knockdown of L1CAM in neocortical PyNs does not affect average AIS length or area. Quantification of average AIS length (C) and area (D) of GFP+ and GFP- PyNs in layer II of the somatosensory cortex from CD1 mice electroporated at E15.5 with plasmids expressing EGFP and shL1CAM#1 and sacrificed at P28. 38-40 AISs (C) and 14-15 AISs (D) from 3 animals were analyzed for each condition; Student's t tests. In (C) and (D), AnkG immunostaining was used for the visualization and morphological analysis of GFP+ and GFP- PyN AISs.
(E) Western blot of total lysates from DIV14 primary cortical neurons infected at DIV3 with lentiviruses expressing shCtrl, shL1CAM#1, or shL1CAM#2, probed with antibodies to AnkG, L1CAM, and γ-tubulin. Data shown are representative of three independent experiments. As indicated, the relative amount of AnkG protein levels normalized to γ-tubulin protein levels are similar across knockdown conditions.
(F) Quantification of the average number of ChC cartridges per single RFP+ ChC under PyN L1CAM or control knockdown conditions at P28. Brain slices (50 μm thickness) were prepared from *Nkx2.1-CreER;Ai9* mice electroporated at E15.5 with plasmids expressing EGFP and shCtrl or shL1CAM#1 and sacrificed at P28. Confocal images were acquired and the average number of ChC cartridges was then calculated for single ChCs in 200 μm x 200 μm fields of view in the somatosensory cortex. 10 ChCs from 3 animals were analyzed for each condition; Student's t test.
(G) Quantification of the percentage of GFP+ PyNs innervated at their AIS, somatodendritic compartment, or distal axon (> 50 μm away from soma) by single RFP+ ChCs at P28. Innervation percentages are indicated for each condition (in Fig. S3G and H). 10 ChCs and 18-53 GFP+ PyNs per ChC from 3 animals were analyzed for each condition; Student's t tests.
(H) Quantification of the percentage of GFP- or GFP+ and GFP- PyN AISs innervated by single RFP+ ChCs at P28. 10 ChCs and 102-210 PyN AISs per ChC from 3 animals were analyzed for each condition; Student's t tests.
n.s. indicates $p \geq 0.05$, ***$p < 0.001$. Data are mean ± SEM.

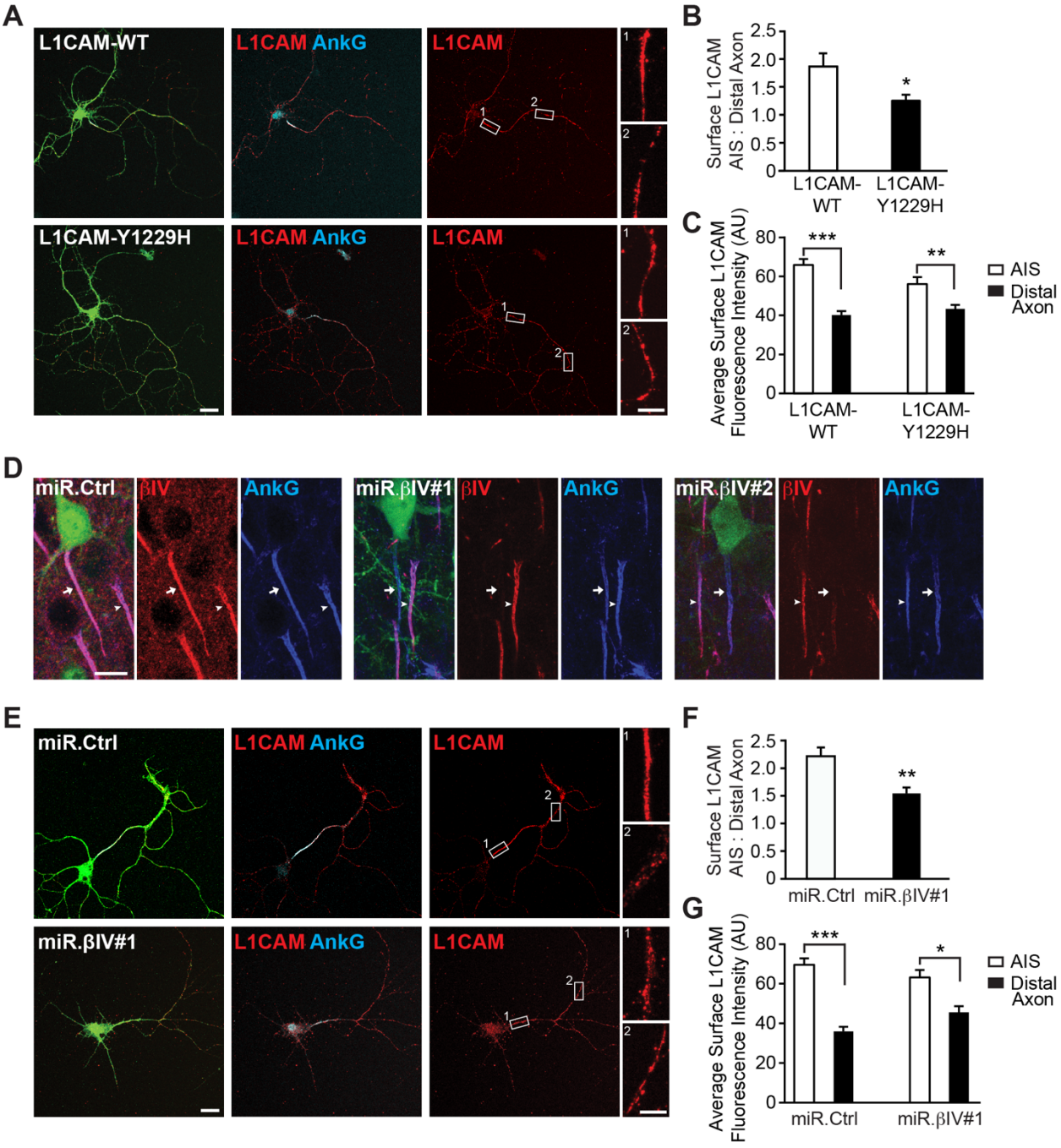

Figure S4. Disrupting L1CAM's Interaction with the AnkG-βIV-spectrin AIS Cytoskeletal Complex Perturbs the Subcellular Distribution of Surface L1CAM. Related to Figure 6.

(A-C) Disrupting PyN L1CAM-AnkG interaction reduces levels of surface L1CAM at the AIS relative to the distal axon. (A) Representative images of surface labeling of L1CAM (red) in DIV10 cultured cortical neurons transfected at E15.5 (DIV0) with plasmids expressing EGFP and L1CAM-WT or an AnkG-binding deficient mutant L1CAM-Y1229H. Scale bar, 10 µm. Enlarged views of boxed areas (right) depict surface L1CAM on the AIS (1) or distal axon (2) (within a region of the axon spanning approximately 40 µm from the AIS). Scale bar, 5 µm. (B)

Quantification of the ratio of average surface L1CAM fluorescence intensity at the AIS versus distal axon in DIV10 cultured cortical neurons. (C) Quantification of the average fluorescence intensity (AU) of surface L1CAM at the AIS or distal axon in DIV10 cultured cortical neurons. For (B) and (C), 35-40 neurons from 3 independent cultures (from at least 3 individual animals) were analyzed for each condition; Student's t tests.

(D) Validation of shRNAs against βIV-spectrin. Representative images of PyNs in layer II of the somatosensory cortex from CD1 mice electroporated at E15.5 with plasmids expressing EGFP and CAG-driven miR30-based shRNAs targeting βIV-spectrin (miR.βIV#1 or miR.βIV#2) or miR.Ctrl and sacrificed at P28. Endogenous βIV-spectrin is visualized by immunostaining for βIV-spectrin (red). GFP+ miR.βIV#1- or miR.βIV#2-, but not miR.Ctrl-, expressing PyNs have reduced βIV-spectrin levels at their AIS (arrows) compared to neighboring GFP- PyNs (arrowheads). Scale bar, 10 μm.

(E-G) PyN βIV-spectrin knockdown reduces levels of surface L1CAM at the AIS relative to the distal axon. (E) Representative images of surface labeling of L1CAM (red) in DIV10 cultured cortical neurons transfected with plasmids expressing EGFP and miR.βIV#1 or miR.Ctrl. Scale bar, 10 μm. Enlarged views of boxed areas (right) depict surface L1CAM on the AIS (1) or distal axon (2) (within a region of the axon spanning approximately 40 μm from the AIS). Scale bar, 5 μm. (F) Quantification of the ratio of average surface L1CAM fluorescence intensity at the AIS versus distal axon in DIV10 cultured cortical neurons. (G) Quantification of the average fluorescence intensity (AU) of surface L1CAM at the AIS or distal axon in DIV10 cultured cortical neurons. For (F) and (G), 39-43 neurons from 3 independent cultures (from at least 3 individual animals) were analyzed for each condition; Student's t tests.

*$p < 0.05$, **$p < 0.01$, ***$p < 0.001$. Data are mean ± SEM.

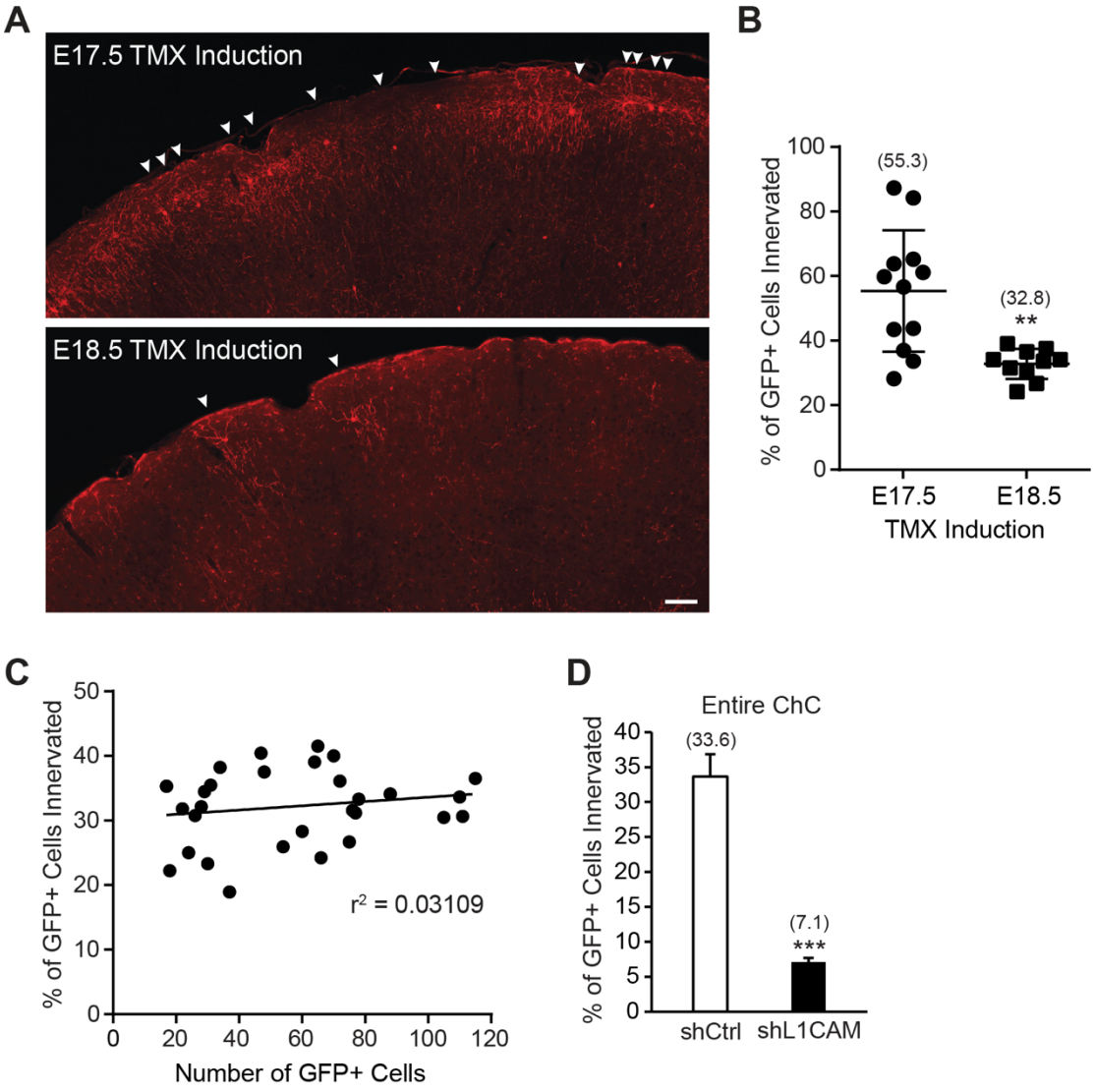

Figure S5. Number of Genetically Labeled ChCs, but Not the Number of Electroporated PyNs, Affects Quantification of ChC/PyN AIS Percent Innervation and PyN L1CAM Knockdown Innervation Phenotype is Recapitulated in Analysis of Serially Reconstructed RFP+ ChCs. Related to Figures 1-6.

(A) Representative images of RFP+ ChCs in layer II of the somatosensory cortex from *Nkx2.1-CreER;Ai9* mice induced with tamoxifen (TMX) at E17.5 or E18.5 and sacrificed at P28. Arrowheads indicate RFP+ ChCs. Composite images; scale bar, 100 µm.

(B) Quantification of the percentage of GFP+ PyNs innervated by RFP+ ChCs at P28. Innervation percentages are indicated for each condition (in Fig. S5B and D). 10-12 ChCs and 38-142 GFP+ PyNs per ChC from 3 animals were analyzed for each condition; Student's t test.

(C) Scatter plot illustrating that the percentage of GFP+ PyNs innervated by single RFP+ ChCs is not related to the number of GFP+ PyNs present in each field of view. 29 ChCs and 17-111 GFP+

PyNs per ChC from 8 animals were analyzed; Pearson correlation, $r^2 = 0.031$, $p = 0.343$.
(D) Quantification of the percentage of GFP+ PyNs innervated by entire single RFP+ ChCs at P28. Serial reconstructions of entire individual RFP+ ChCs and all neighboring GFP+ PyNs were analyzed to quantify total ChC/PyN AIS percent innervation. 8-10 ChCs and 74-630 GFP+ PyNs per ChC from 3 animals were analyzed for each condition; Student's t test.
**$p < 0.01$, ***$p < 0.001$. Data are mean ± SEM.

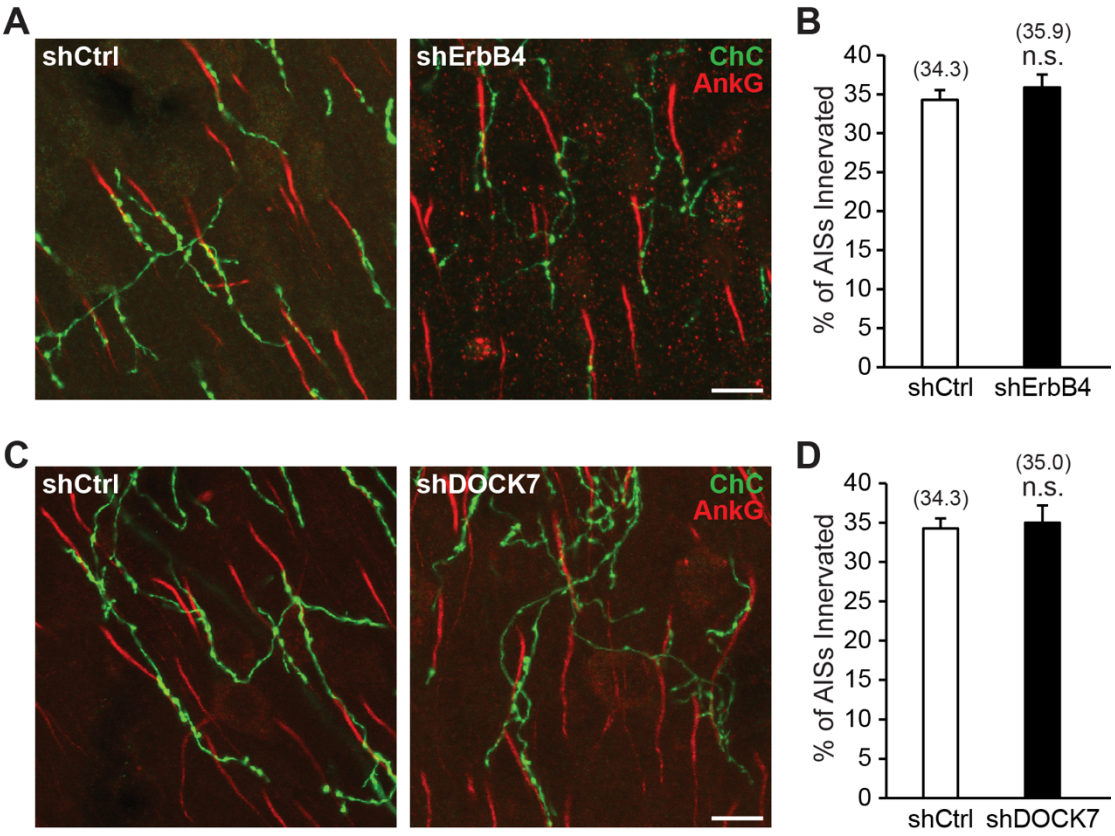

Figure S6. Knockdown of ChC-expressed ErbB4 or DOCK7 Does Not Affect Neocortical ChC/PyN AIS Percent Innervation. Related to Figure 3.

(A) Representative images of GFP+ ChCs in layer II of the somatosensory cortex from CD1 mice subjected to vMGE-directed IUE at E13.5 with plasmids expressing EGFP and shCtrl or shErbB4 and sacrificed at P28. Scale bar, 10 µm.

(B) Quantification of the percentage of PyN AISs innervated by single GFP+ ChCs at P28. Innervation percentages are indicated for each condition (in Fig. S6B and D). 8 ChCs and 114-271 PyN AISs per ChC from 3 animals were analyzed for each condition; Student's t test.

(C) Representative images of GFP+ ChCs in layer II of the somatosensory cortex from CD1 mice subjected to vMGE-directed IUE at E13.5 with plasmids expressing EGFP and shCtrl or shDOCK7 and sacrificed at P28. Scale bar, 10 µm.

(D) Quantification of the percentage of PyN AISs innervated by single GFP+ ChCs at P28. 8 ChCs and 105-275 PyN AISs per ChC from 3 animals were analyzed for each condition; Student's t test. n.s. indicates $p \geq 0.05$. Data are mean ± SEM.

Table S1: PyN-expression of Candidate Cell Surface Molecules. Related to Figure 2.

Cell Surface Molecule	Neocortical PyN		Embryonic Expression	Postnatal/Adult Expression	References
	Axonal Expression	AIS Enriched (Total Protein)			
NF186	✓	✓	✓	✓*	(Hedstrom et al., 2007); (Kriebel et al., 2011)
NrCAM	✓	✓	✓*	✓*	(Hedstrom et al., 2007)
L1CAM	✓	–	✓*	✓*	(Boiko et al., 2007); (Scotland et al., 1998)
CHL1	✓	–	✓*	✓*	(Demyanenko et al., 2011)
TAG-1	✓	✓	✓*	✓*	(Ogawa et al., 2008)
SCN1B	✓	✓	✓	✓*	(Wimmer et al., 2015)
ADAM22	✓	✓	–	✓*	(Ogawa et al., 2010)
CASPR2	✓	✓	✓	✓*	(Inda et al., 2006); (Ogawa et al., 2008)
EphA3	✓	–	✓*	✓*	(Nishikimi et al., 2011)
EphA4	✓	–	✓*	✓*	(Greferath et al., 2002)
EphB2	✓	–	✓*	✓*	(Cisse et al., 2011)
EfnB1	✓	–	✓*	✓*	(McClelland et al., 2009)
EfnB2	✓	–	✓*	✓*	(McClelland et al., 2009)
EfnB3	✓	–	✓*	✓*	(Xu and Henkemeyer, 2009)

✓ = Yes/Present – = No/Absent * Allen Brain Atlas

Table S2: RNAi Targeting Sequences. Related to Key Resources Table in the STAR Methods Section.

REAGENT or RESOURCE	SOURCE	IDENTIFIER
Oligonucleotides		
shRNA targeting sequence: Ctrl: GCTATACGGGATCGAAAGA	(Watabe-Uchida et al., 2006)	N/A
shRNA targeting sequence: mouse L1CAM#1: GCATCCACTTCAAACCCAA	This paper	N/A
shRNA targeting sequence: mouse L1CAM#2: AGCCTTACCAGAAGGGAAA	This paper	N/A
shRNA targeting sequence: mouse NrCAM: GCAATGCCTCTAACAAATA	This paper	N/A
shRNA targeting sequence: mouse TAG-1: CCTGCTTTGCTGAGAACTT	This paper	N/A
shRNA targeting sequence: mouse CASPR2: GATTAGAGCCAGAGGGAAT	(Anderson et al., 2012)	N/A
shRNA targeting sequence: mouse EphA3: GGACCTATGTTGATCCACATA	(Nishikimi et al., 2011)	N/A
shRNA targeting sequence: mouse EphA4: GCAGCACCATCATCCATTG	(Khodosevich et al., 2011)	N/A
shRNA targeting sequence: mouse EphB2: ACGAGAACATGAACACTAT	(Cisse et al., 2011)	N/A
shRNA targeting sequence: mouse EfnB1: CACTGTGCTTGATCCCAAT	(McClelland et al., 2009)	N/A
shRNA targeting sequence: mouse EfnB2: GCAGACAGATGCACAATTA	(McClelland et al., 2009)	N/A
shRNA targeting sequence: mouse EfnB3: GCCTTCGGAGAGTCGCCAC	(McClelland et al., 2009)	N/A
shRNA targeting sequence: mouse ErbB4: CCAGACTACCTGCAGGAATAC	(Tai et al., 2014)	N/A
shRNA targeting sequence: mouse DOCK7: GGTACAGTACACATTTACA	(Tai et al., 2014)	N/A
miR30 targeting sequence: Ctrl: AGGAATTATAATGCTTATCTA	This paper	N/A
miR30 targeting sequence: mouse L1CAM: GAGAATCAACGGAATGTCTAA	This paper	N/A
miR30 targeting sequence: mouse CHL1: TACCAGGATAGAGGAAATTAA	This paper	N/A
miR30 targeting sequence: mouse NF186#1: CACCAGTCAATGCCATCTATA	This paper	N/A
miR30 targeting sequence: mouse NF186#2: CACGATCTCGGTGAGAGTAAA	This paper	N/A

miR30 targeting sequence: mouse ADAM22: ACATGGCAGATGTGATCTATA	This paper	N/A
miR30 targeting sequence: mouse SCN1B: GTCTACCGTCTCCTCTTCTTA	This paper	N/A
miR30 targeting sequence: mouse βIV-Spectrin#1: CAGGAGAAATTCTCAGAGTTA	This paper	N/A
miR30 targeting sequence: mouse βIV-Spectrin#2: GACCACGATCGAGAAACTCAA	This paper	N/A
Forward Primer: hL1CAM-F: AGAATTCATGGTCGTGGCGCTGCGGTAC	This paper	N/A
Reverse Primer: hL1CAM-R: AGCTTTGTTTAAACCTTCTAGGGCCACGGC AGGGTTG	This paper	N/A